ELSEVIER

Thermochimica Acta 290 (1996) 123–132

thermochimica acta

Thermal decomposition of ammonium trioxalatoferrate(III) trihydrate in air

El-H.M. Diefallah [a,*], S.N. Basahel [a], A.A. El-Bellihi [b]

[a] *Chemistry Department, Faculty of Science, King Abdulaziz University, Jeddah, P.O. Box 9028, Saudi Arabia*

[b] *Chemistry Dept., Faculty of Science, Zagazig University, Benha-Branch, Benha, Egypt*

Received 20 October 1995; accepted 14 April 1996

Abstract

The thermal decompostition of ammonium trioxalatoferrate(III) trihydrate in air has been studied using DTA–TG, electrical conductivity, SEM, XRD, FTIR and Mössbauer effect measurements. The first stage of decomposition of $(NH_4)_3[Fe(C_2O_4)_3]\cdot 3H_2O$, starting at about 100°C, corresponds to evolution of the water of hydration and is followed by the second stage in which the sample ignites at around 260°C and burns rapidly to form finely divided iron(III) oxide. DC-electrical conductivity measurements showed two breaks corresponding to the two decomposition stages. Kinetic analysis of the two stages of the decomposition reactions was performed under isothermal conditions and the results were compared with those obtained under non-isothermal conditions using different integral methods of analysis. The fractional reaction–time data showed a sigmoid relationship and obeyed the Avrami–Erofeev equation characteristic of a solid-state nucleation-growth mechanism and consistent with the textural changes that accompany the decomposition, as revealed by SEM experiments. Mössbauer spectra of samples calcined at different temperatures are discussed and show that in the early stages of the decomposition at about 300°C, part of the Fe(III) oxide is formed in a superparamagnetic doublet state. As the temprature is increased, the crystallites grow and supermagnetism disappears..

Keywords: Ammonium trioxalatoferrate(III); Decomposition; DTA; ESM; Mössbauer; TG

1. Introduction

The use of Mössbauer spectroscopy, in addition to thermoanalytical techniques, to study the reactions and thermal decomposition of solids under different conditions, has been very useful, especially in following changes and in the identification of the chemical states of the products. For example, Gallagher and co-workers [1] used the Mössbauer effect to monitor changes in the oxidation of iron associated with the thermal decomposition of alkaline earth trisoxalatoferrate(III), and the reduction of europium followed by subsequent reoxidation during the thermal decomposition of europium(III) oxalate. The thermal decomposition of rare earth hexacyanoferrate(III) and ammonium hexacyanoferrate(II) in air or oxygen has been demonstrated to be a good technique for the preparation of

* Corresponding author.

PII S0040-6031(96)03015-8

rare earth orthoferrites [2]. More recently, the Mössbauer effect has been used to investigate catalytic processes, surface structure and reactions at solid surfaces [3,4]. The examination of microcrstallites adsorbed onto high-area inert supports has been found to be useful in such investigations. Their Mössbauer parameters were found to depend on particle size and distribution, which depend on the extent of calcination. The differences in chemical isomer shifts and quadrupole splittings produced by particles of different sizes were temperature-dependent and were associated with the number of defects in the crystal structure. Smaller particles gave larger quadrupole splittings, whereas larger particles gave six-line spectra characteristic of magnetically ordered, bulk α-Fe_2O_3.

There is considerable diversity in the mechanisms by which solids react and there are a variety of factors which may control, determine, influence or modify the rate-limiting processes [5]. The kinetics of the thermal decomposition of solids are affected by experimental factors and processing parameters [6,7]. Moreover, the use of different methods of kinetic analysis of isothermal and dynamic TG data obtained on one system usually gives different results [8]. The kinetics and mechanism of the thermal decomposition of simple metal oxalates have attracted the interest of several investigators [9]. However, relatively few studies on the kinetics of the thermal decomposition reactions of oxalato complexes have been reported [10,11]. In the present study,the thermal decomposition of ammonium trisoxalatoferrate(III) trihydrate in air has been studied using differential thermal analysis–thermogravimetry (DTA–TG), DC-electrical conductivity, scanning electron microscopy (SEM), X-ray diffractometry (XRD), Fourier transform infrared (FTIR) and Mössbauer effect measurements. Kinetic analyses of isothermal and dynamic TG data were performed and considered with reference to the various models and computational methods of solid-state reactions [8,12–14]. The temperature dependence of the DC-electrical conductivity of the oxalate complex, and the XRD,SEM,FTIR and Mössbauer effect of samples calcined at different temperatures were measured. The results of the various techniques used to examine the chemical phase, morphology and texture changes that occur during the thermal decomposition and the kinetics of the decomposition reactions are compared and discussed.

2. Experimental

The compound $(NH_4)_3[Fe(C_2O_4)_3]\cdot 3H_2O$ was prepared as described in the literature [15].

Simultaneous DTA–TG experiments were performed using a Shimadzu DT 40 thermal analyzer. The experiments were performed under isothermal conditions or at the different specified heating rates in air at a flow rate of 3.0 Lh^{-1}. The sample mass in the Pt cell of the thermal analyzer was kept at about 8 mg in all experiments, in order to ensure a linear heating rate and accurate temperature measurements.

DC-electrical conductivity measurements were made on pellets using a two-probe method with Cu electrodes. Pellets of 1.3 cm diameter and 0.2 cm thickness were prepared by cold pressing powder under a pressure equal to 2.2×10^3 kg cm^{-2}. Silver paste was used as the electrode which showed ohmic contact with the sample. A Keithley electrometer type 610 C was used for measuring the electric current. The measurements were carried out in air in the temperature range 25–300°C. A copper–constantan thermocouple was used for recording the sample temperature.

Samples of ammonium trioxalatoferrate(III) trihydrate were inserted into an electric oven at room temperature and the temperature was raised to the desired value, which was maintained for 30 min before the sample was removed and cooled in air in a desiccator to room temperature. Mössbauer spectra of the samples calcined at the different temperatures were determined at room temperature relative to iron foil, using an MS 900 Ranger Scientific Co. Mössbauer Spectrometer with ^{57}Co source in metallic iron. The changes in morphology and texture taking place during the thermal decomposition of the salt were investigated using a Jeol T 300 scanning electron microscope. X-ray diffraction patterns for the calcined samples were recorded with a Philips PW 1710 X-ray diffraction unit using a Cu target and a Ni filter. Fourier transform infrared spectra of the calcined samples were recorded using a Shimadzu FTIR-8101 spectrophotometer.

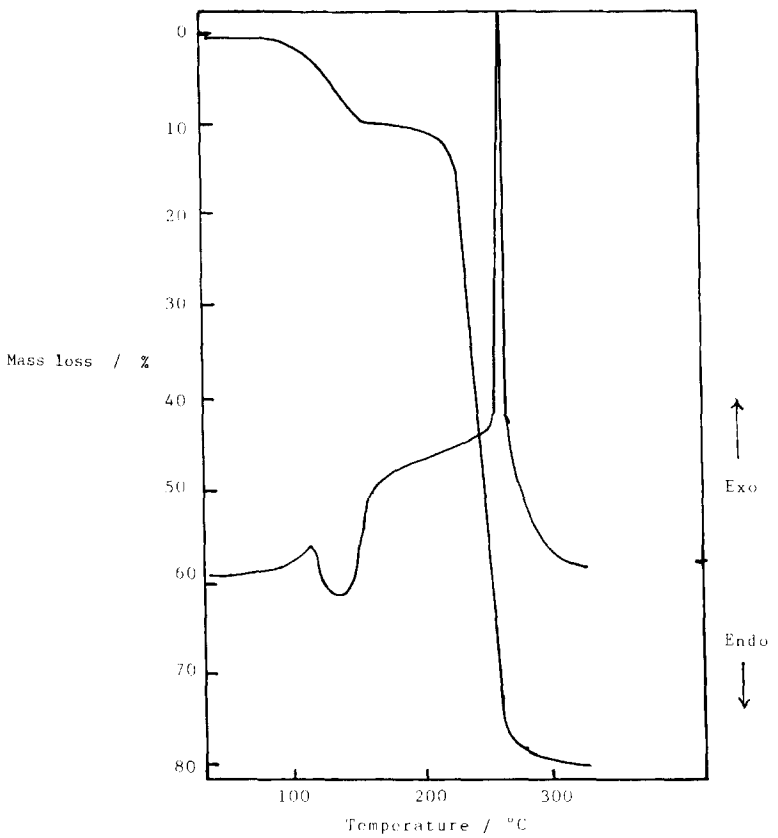

Fig. 1. DTA–TG curves of $(NH_4)_3[Fe(C_2O_4)_3 \cdot 3H_2O$ in air.

3. Results and discussion

Fig. 1 shows the DTA–TG curves obtained for $(NH_4)[Fe(C_2O_4)] \cdot 3H_2O$ in air. The results are in general agreement with previous investigations [16]. The DTA curve shows one broad endothermic peak at about 130°C, due to dehydration, and a sharp exothermic peak at 260°C due to decomposition and oxidation of the anhydrous complex salt to iron(III) oxide. The TG curve also showed two steps due to dehydration and decomposition, and both steps are smooth with no inflexion points. The mass changes observed on the TG trace correspond closely to the peaks in the DTA curve. In nitrogen, however, an inflexion was observed at 375°C and 66.5% mass loss, corresponding to the formation of the anhydrous ferrous oxalate [16]. Fig.2 shows how the DC-electrical conductivity of the sample changes with temperature. There are two breaks which mark the two stages observed in the DTA–TG results. The room temperature conductivity values are close to that of pure water. Thus, the conduction process in the hydrate is expected to be through the water molecules. The dependence of conductivity on temperature is due to changes in the type and concentration of the contributing carriers accompanying the chemical and phase changes during the thermal decomposition. Generally, the conductivities lie in the semiconductor range and increase rapidly with temperature on dehydration and decomposition of the complex to iron(III)oxide.

Mössbauer spectra at room temperature of samples calcined at different temperatures are shown in Fig.3. The spectrum of the hydrate $(NH_4)_3[Fe(C_2O_4)_3] \cdot 3H_2O$ prior to calcination (curve(a)) shows an isomer shift of 0.24 mm s^{-1}. For

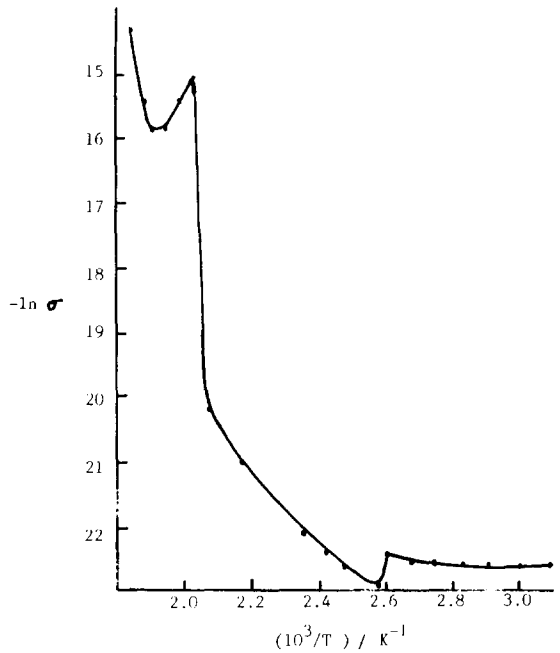

Fig. 2. Temperature dependence of the electrical conductivity (σ) of ammonium trioxalatoferrate(III) trihydrate.

samples calcined at 90°C, the complex was partially dehydrated with broadening of the Mössbauer line (curve(b)). Upon increasing the calcination temperature to 200°C, curve(c) shows a quadrupole splitting with $\Delta E_Q = 0.84$ and $\delta = 0.38$ mm s^{-1}. These values are in good agreement with the values reported by Brady and Duncan [17] for ammonium trioxalatoferrate(III). At about 300°C, the calcination product (curve (d)), consisted of two Fe(III) oxides, one with a superparamagnetic doublet ($\Delta E_Q = 0.54$ mm s^{-1}), having an isomer shift ($\delta = 0.16$ mm s^{-1}) associated with trivalent iron and indicating that the particles are finely divided or amorphous, while most of the Fe_2O_3 formed had a six-fold spectrum due to the large particle size [2,3]. The spectrum exhibits a magnetic hyperfine splitting of 491 kOe which is significantly less than the normal value for iron(III) oxide of 515 kOe. At 400°C, the Mössbauer spectrum (curve (e)) shows a hyperfine splitting of 516 kOe and the supermagnetism disappears, thus giving rise to the characteristic spectrum of Fe_2O_3 with the larger particle size.

SEM micrographs showing the changes in morphology and texture that accompany the salt decomposition are shown in Fig. 4. Each sample was calcined for about 30 min at the specified temperature. The results show that the particle shape and size change throughout the decomposition. SEM micrographs of the parent material at room temperature show joined and irregularly-shaped crystals of different sizes (Fig. 4a). Micrographs of samples calcined at 210°C (Fig. 4b) which had undergone dehydration show superficial roughening and rounding of crystal edges. The decomposition of $(NH_4)_3[Fe(C_2O_4)_3]$ at 280–300°C produced a large number of small and fine granules (Fig. 4c). The product obtained rapidly absorbs moisture from the air and turns reddish-brown. The SEM micrograph of a sample calcined at about 300°C shows a gelatinous appearance (Fig. 4d) due to absorption of moisture from the atmosphere. At 400°C, the fine grains were re-textured into aggregates of crystallites (Fig. 4e) showing smooth surfaces and some irregularities of shape. Above 600°C, the crystallites coalesced to form black regular trigonal symmetrical crystalline structures with sharp edges and angles characteristic of α-Fe_2O_3 oxide (Fig. 4f).

The results of SEM and the Mössbauer experiments are consistent with the results of XRD and FTIR analysis. Samples calcined at 400 and 600°C gave XRD patterns of α-Fe_2O_3, whereas samples calcined at 280–300°C showed none of the XRD lines characteristic of iron(III) oxide crystallites. This provides evidence that the oxide formed in this temperature range is microcrystalline (or possibly even amorphous) as suggested by SEM and Mössbauer experiments. FTIR spectra of samples calcined at 280, 300, 400 and 600°C were similar and characteristic of iron(III) oxide. The results of SEM,XRD,FTIR and Mössbauer experiments are consistent and suggested that the product oxide formed at about 280–300°C is microcrystalline and has a high surface area. The decomposition of the corresponding chromium oxalate complex, $(NH_4)_3[Cr(C_2O_4)_3]$, at 350°C in air leads to non-stoichiometric chromium oxides amorphous to X-rays [18].

The isothermal α–t curves for dehydration and decomposition of the complex (shown in Fig. 5)

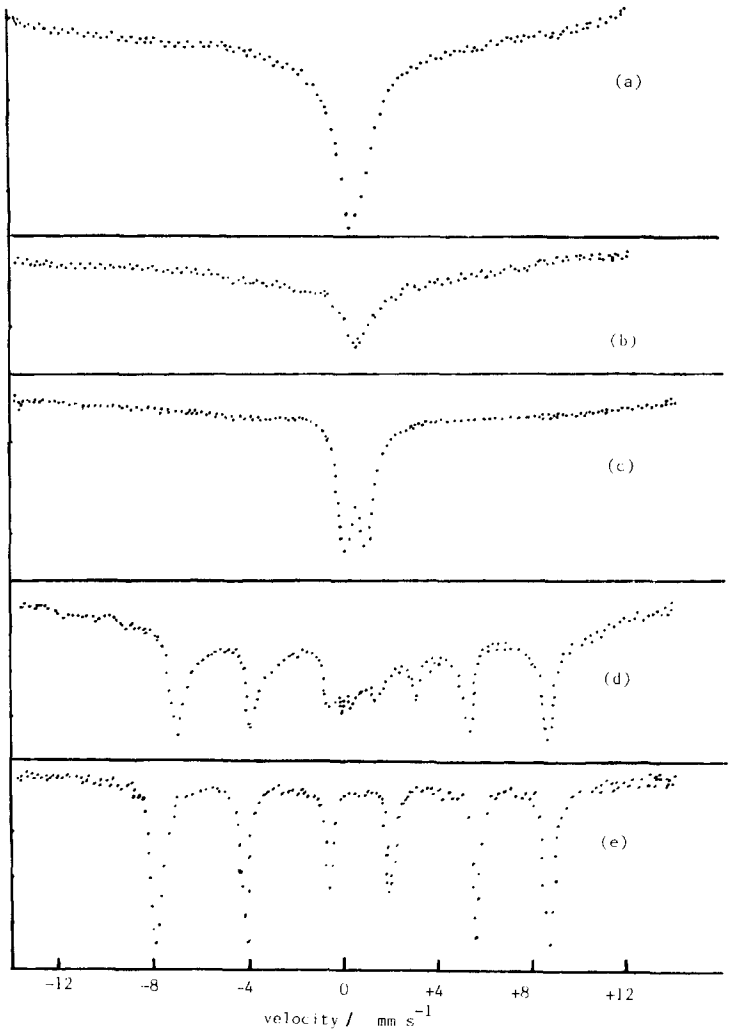

Fig. 3. Mössbauer spectra of ammonium trioxalatoferrate(III) trihydrate, calcined at different temperatures: (a) ambient temperature; (b) 90; (c) 200; (d) 300 and (e) 400°C.

were analysed in terms of the theoretical solid-state reaction equations [8,12–14]. The curves have the sigmoid shape characteristic of autocatalytic solid-state reactions. Kinetic analysis of isothermal data showed that the results are best described by the Avrami–Erofeev A_2 and A_3 models [14], in which the reaction is controlled by initial random nucleation followed by overlapping growth in two and three dimensions. The fine-grained decomposition products formed in the early stages of the decomposition catalyses the reaction as it proceeds. Kinetic analysis of the data showed best fit and minimum deviations with the nucleation and growth rate equations, thus giving support to this model. the diffusion and other heterogeneous reaction kinetic models have gave a less satisfactory fit to the experimental results.

Under non-isothermal conditions and with the heating rate set to a constant value β, the kinetic model function $g(\alpha)$ is given by Doyle's equation [19]

$$g(\alpha) = \frac{A}{\beta}\int_0^T \exp\left(-\frac{E}{RT}\right)\mathrm{d}T = \frac{AE}{R\beta}P(x)$$

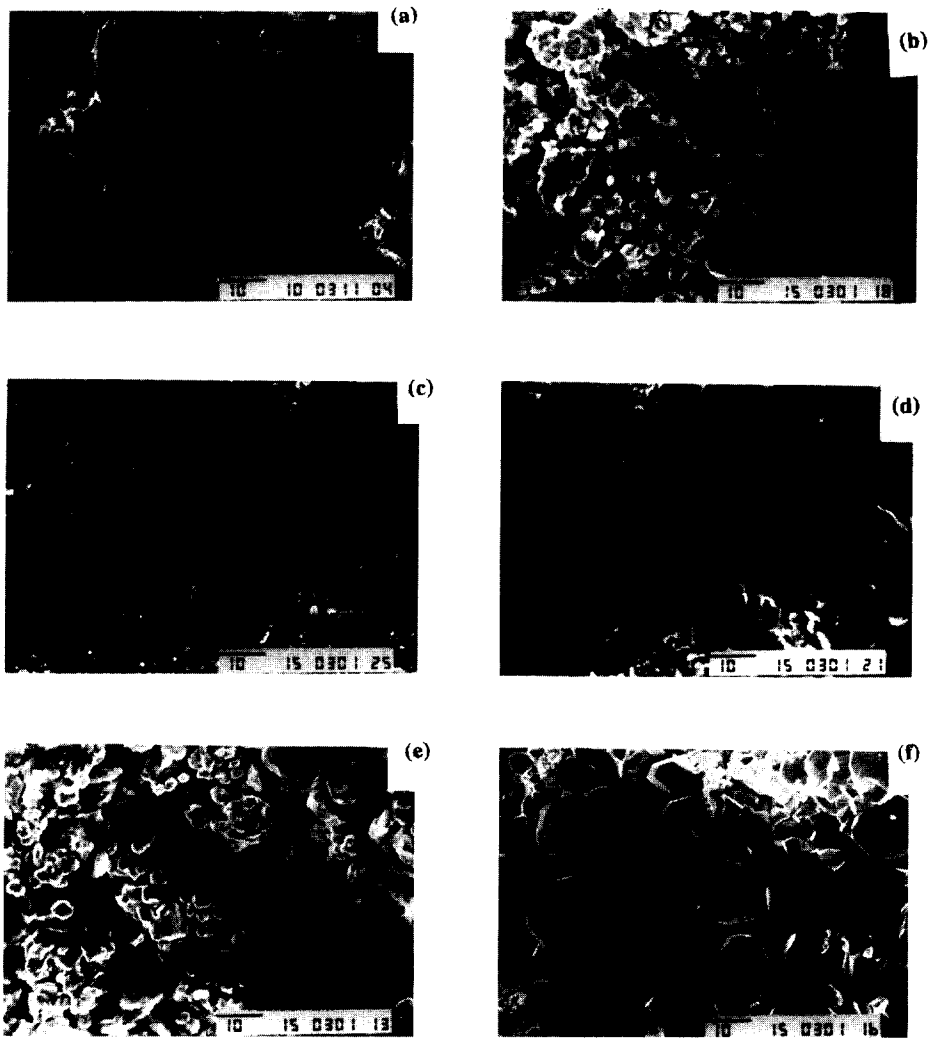

Fig. 4. Scanning electron micrographs showing the changes in texture and morphology that accompany the thermal decomposition of ammonium trioxalatoferrate(III) trihydrate in air. (a) Parent compound at room temperature showing relatively large crystals of different sizes and shapes. (b) Sample calcined at 210°C after loss of water of hydration showing breaking into small crystallites and roughening of crystal surfaces. (c) Sample calcined at 280°C showing degradation to small and fine granules. (d) sample calcined at 300°C, after absorption of moisture from the atmosphere, showing shapeless and gelatinous appearance. (e) Sample calcined at 400°C showing re-texturing into aggregates of crystallites. (f) Sample calcined at 600°C showing grown trigonal crystals with sharp edges and angles. (Scale bar 10 μm)

The function $P(x)$ has been defined as

$$P(x) = \frac{e^{-x}}{x} - \int_0^{\infty} \frac{e^{-u}}{u} du$$

where $u = E/RT$ and x is the corresponding value of u at which a fraction α of material has decomposed. In the Coats–Redfern method [20], the function $g(\alpha)$ is approximated to the form

$$g(\alpha) = \frac{ART^2}{\beta E}\left[1 - \frac{2RT}{E}\right] e^{-E/RT}$$

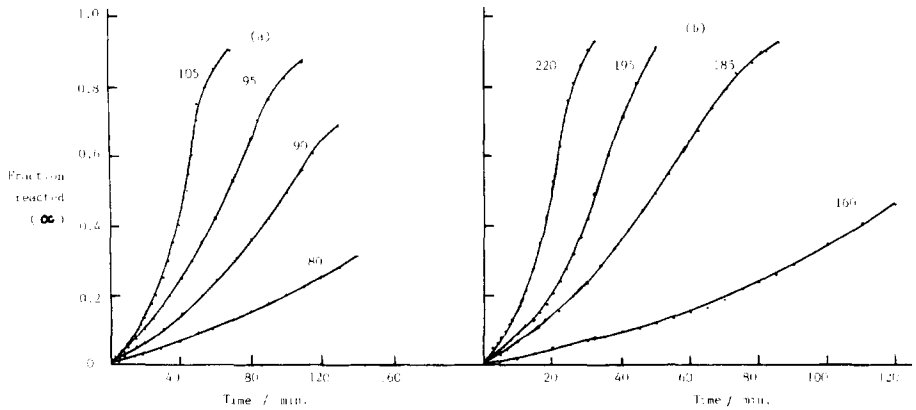

Fig. 5. Isothermal α/t curves for the decomposition of ammonium trioxalatoferrate(III) trihydrate in air: (a) dehydration ; (b) decomposition of the anhydrous complex to iron(III) oxide.

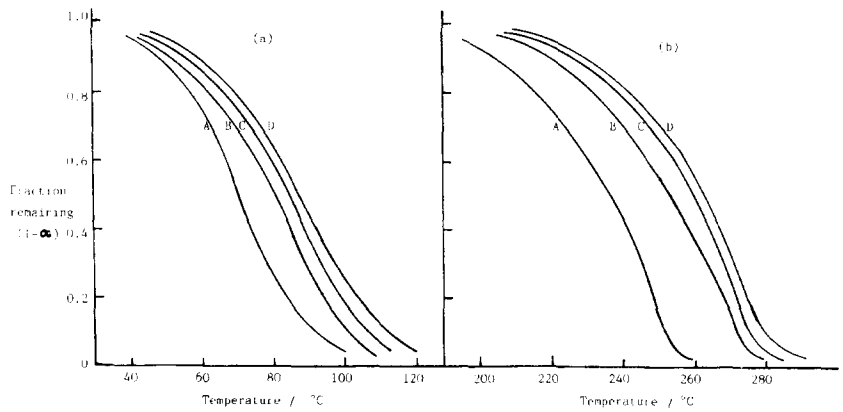

Fig. 6. Dynamic measurements for the decomposition of ammonium trioxalatoferrate(III) trihydrate in air: (a) dehydration ; (b) decomposition of the anhydrous complex to iron(III) oxide. Heating rate: curve A, 10°C min^{-1}; curve B, 15°C min^{-1}; curve C, 20°C min^{-1}; and curve D, 25°C min^{-1}.

This equation has been written in the form

$$-\ln\left[\frac{g(\alpha)}{T^2}\right] = -\ln\frac{AR}{\beta E}\left(1-\frac{2RT}{E}\right)+\frac{E}{RT}$$

The quantity $\ln(AR/\beta E)(1-(2RT/E))$ is reasonably constant for most values of E and in the temperature range over which most reactions occur. In the Ozawa method [21], a master curve has been derived from the TG data obtained at different heating rates (β) using Doyle's equation and assuming that $[(AE/R\beta)P(E/RT)]$ is a constant for a given fraction of material decomposed. The function $P(E/RT)$ was approximated by the equation

$$\log P\left(\frac{E}{RT}\right) = -2.315-0.4567\left(\frac{E}{RT}\right)$$

so that

$$-\log\beta = 0.4567\left(\frac{E}{RT}\right)+\text{constant}$$

Hence, the activation energy is calculated from the thermogravimetric data obtained at different heat-

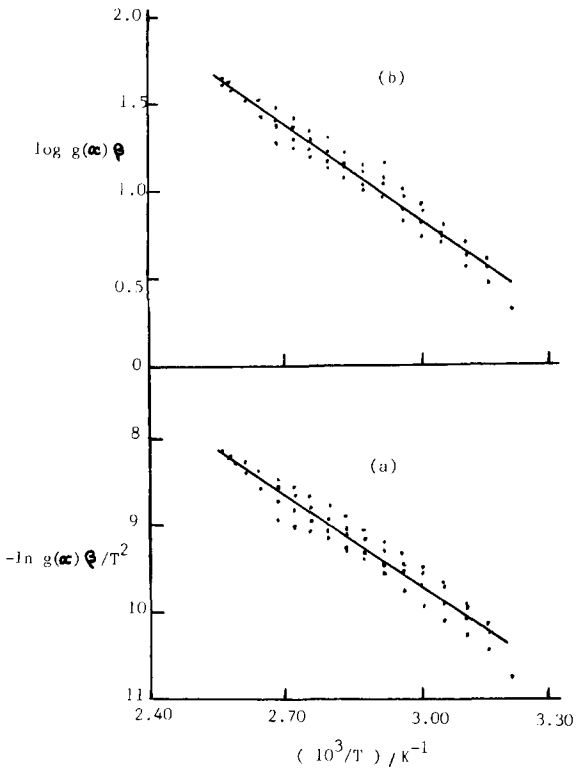

Fig. 7. Composite analysis of the dynamic dehydration of ammonium trioxalatoferrate(III) trihydrate based on (a) the modified Coats–Redfern equation (Composite I) and (b) Doyle's equation (Composite II), assuming the A_2 model.

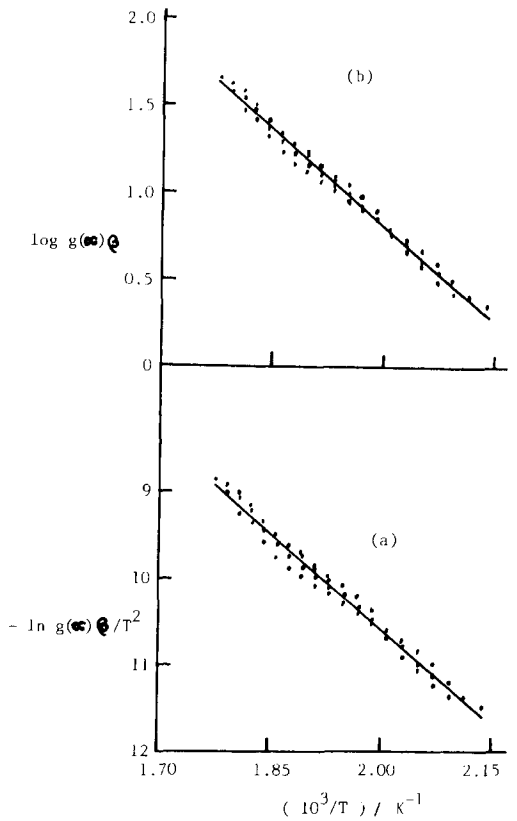

Fig. 8. Composite analysis of the dynamic decomposition of ammonium trioxalatoferrate(III) based on (a) the modified Coats–Redfern equation (Composite I) and (b) Doyle's equation (Composite II) assuming the A_2 model.

ing rates. The frequency factor is calculated from the equation

$$\log A = \log g(\alpha) - \log\left[\frac{E}{\beta R}P\left(\frac{E}{RT}\right)\right]$$

It is obvious that the calculation of E is independent of the reaction model used to describe the reaction, whereas the frequency factor depends on the determined form of $g(\alpha)$.

In the composite method of analysis of dynamic data [8], the results obtained not only at different heating rates, but also with different α values, are superimposed on one master curve. This can be achieved by two equivalent methods, either by use of the modified Coats–Redfern equation [20] (composite I) or Doyle's equation [19] (composite II). In composite method I, the modified Coats–Redfern equation is written in the form

$$\ln\left[\frac{\beta g(\alpha)}{T^2}\right] = \ln\left(\frac{AR}{E}\right) - \frac{E}{RT}$$

Hence, the dependence of $\ln[(\beta g(\alpha)/T^2)]$, calculated for different α values at their respective β values, on $1/T$ must give rise to a single master straight line for the correct form of $g(\alpha)$, and a single activation energy and frequency factor can be readily calculated. In composite method II, Doyle's equation is rewritten in the form

$$\log g(\alpha)\beta = \left[\log\frac{AE}{R} - 2.315\right] - 0.4567\frac{E}{RT}$$

Again, the dependence of $\log g(\alpha)\beta$, calculated for

Table 1
Activation parameters of the thermal dehydration and decomposition of $(NH_4)_3[Fe(C_2O_4)_3]\cdot 3H_2O$ calculated according to the A_2 model.

Method of analysis	Dehydration step		Decomposition step	
	E/kJ mol^{-1}	$\log_{10} A$/min^{-1}	E/kJ mol^{-1}	$\log_{10} A$/min^{-1}
Isothermal	25±5	3.0±0.7	63±3	5.7±0.3
Non-isothermal				
(a) Coats–Redfern	28±2	3.8±0.4	62.2±2	5.8±0.3
(b) Ozawa	56±7	8.4±1.1	66±8	6.5±0.4
(c) Composite I	29±1	3.9±0.4	62±1	5.7±0.3
(d) Composite II	33±1	5.0±0.2	67±1	6.5±0.1

the different α values at their respective β values, on $1/T$ must give rise to a single master straight line for the correct form of $g(\alpha)$.

Kinetic analysis of dynamic TG data, shown in Fig. 6, according to the integral methods of Ozawa [21], Coats–Redfern [20] and the composite integral method [8], showed, in general, good agreement between the isothermal results and the results obtained using the different methods of the integral analysis of data. The integral composite analysis of dynamic TG data showed higher correlation and less deviation in the calculated experimental parameters. Figs. 7 and 8 show typical composite plots of non-isothermal data for the dehydration and decomposition steps calculated according to the model. Table 1 shows the results of the activation parameters for the isothermal and non-isothermal study of the two steps calculated according to the A_2 model using different computational methods. The activation parameters for dehydration confirm that the water molecules are lattice water. The activation energy for the decomposition of the anhydrous complex is lower than the values of most normal thermal decomposition chemical reactions, which indicates the autocatalytic action of the fine-grained iron(III) oxide formed in the early stage of the decomposition step as suggested by the Mössbauer effect study.

Acknowledgement

The authors would like to thank Prof. Dr. R.I. Issa for arranging for the Mössbauer experiments at Tanta University Central Lab. and for useful discussions. Thanks are also due to Mr. S. Al-Heniti (Physics Dept. KAU) for doing the XRD, Mr. M. Seif (Production Eng. Dept., KAU) for the SEM and Mr. G. M. Gabr (Chem. Dept., KAU) for doing the FTIR experiments.

References

[1] P.K. Gallagher and C.R. Kurkjian, Inorg Chem., 5 (1966) 214.
P.K. Gallagher, F. Schrey and B. Prescott, Inorg. Chem., 9 (1970) 215.
[2] P.K. Gallagher, and F. Schrey, in R.F. Schwenker, Jr., and P.D. Garn, (Eds.). Thermal Analysis, Vol 2, Academic Press, New York, 1969, p.929.
[3] F.J. Berry, Adv. Inorg. Chem. Radiochem., 21 (1978) 255. L. Lu, W. Hua, X.(1978) 255. Wang, J.G. Stevens and Y. Zhang., Thermochim. Acta, 195 (1992) 389.
[4] F.R. Hartley, Supported Metal Complexes: A New Generation of Catalysts, Reidel, Dordrecht, 1985, p. 1–25.
[5] V.V. Boldyrev, M. Bulens and B. Delmon, the Control of the reactivity of Solids, Elsevier, Amsterdam, 1979.
[6] W.W. Wendlandt, Thermal Methods of Analysis, Wiley-Interscience, New York, 3rd edn., 1976.
[7] P.K. Gallagher and D.W. Johnson, Jr., Thermochim. Acta, 6 (1983) 67.
[8] El-H.M. Diefallah, Thermochim. Acta, 202 (1992) 1.
[9] A.K. Galwey, in H.J. Emeleus (ed.), MTP International Review of Science, Inorganic Chemistry, Series 2, Solid State Chemistry, Vol. 10, Butterworths, London, 1975, p.147.
[10] El-H.M. Diefallah, S.N. Basahel, N.M. El-Fass and E.A. SI-Sabban, Thermochim. Acta, 184 (1991) 141.
[11] J.D. Danforth and J.Dix, Inorg. Chem., 10 (1971) 1623.
[12] S.F. Hulbert and J.J. Klawitter, J. Am. Ceram. Soc., 50 (1967) 484.

[13] J.H. Sharp, G.W. Brindley and B.N.N. Achar, J. Am. Ceram. Soc., 49 (1966) 379.
[14] M.E. Brown, Introduction to Thermal Analysis, Chapman and Hall, New York, 1988, Chapt. 13.
[15] H.L. Saha and S. Mitra, Thermochim. Acta, 112 (1987) 275.
[16] D. Broadbent, D. Dollimore and J. Dollimore, J. Chem. Soc. A, (1967) 451.
[17] P.R. Brady and J.F.Duncan, J. Chem. Soc., 653 (1964).
[18] A. Lerch and A. Rousset, Themochim. Acta, 232 (1994) 233.
[19] C.D. Doyle, J. Appl. Polym. Sci., 5 (1961) 285.
[20] A.W. Coats and J.P. Redfern, Nature, 201 (1964) 68.
[21] T. Ozawa, Bull. Chem. Soc. Jpn., 38, (1965) 1881, J. Therm. Anal., 2 (1970) 301.